RSC Advances

ROYAL SOCIETY OF CHEMISTRY

www.rsc.org/advances

Cite this: DOI: 10.1039/c0xx00000x

www.rsc.org/xxxxxx

ARTICLE TYPE

A green method to gold-graphene nanocomposite from cyclodextrin functionalized graphene for efficient non-enzymatic electrochemical sensing applications

Aswathi R, Mohamed Mukthar Ali, Anurudha Shukla and K. Y. Sandhya*

Received (in XXX, XXX) Xth XXXXXXXXX 20XX, Accepted Xth XXXXXXXXX 20XX
DOI: 10.1039/b000000x

Here, we report a new and green method of synthesis of gold nanoparticle functionalized graphene (Au-Gr) from β-cyclodextrin functionalized Gr (CD-Gr). The CD-Gr, made from CD and reduced graphene oxide (Gr), is dispersible in water and various other solvents and yields individual Gr sheets of ~2 nm thickness in aqueous suspension. The aqueous suspension of CD-Gr on heating with chloroauric acid forms Au-Gr. The CD molecules act as the reducing agent for Au (III) ions to form the Au-Gr. The formation of the Au-Gr is confirmed by various techniques such as UV-visible spectroscopy, scanning and transmission electron microscopy, X-ray diffraction etc. The procedure successfully produces silver functionalized Gr (Ag-Gr) also. The method utilizes just water and CD and hence is benign to environment. The Au-Gr exhibits excellent electrochemical sensing properties with the best detection limit achieved for biomolecules such as glucose and ascorbic acid (AA) with10 and 40 nM, respectively, compared to that reported in the literature by any enzymatic or non-enzymatic electrodes. The excellent sensing property of the Au-Gr is attributed to the synergistic effects of the high conductivity and catalytic activity of Gr and Au, respectively and the better homogeneity, dispersibility, surface area and adsorption achieved due to the presence of CD.

1. Introduction

Graphene (Gr), a novel one-atom-thick two-dimensional carbon system, with excellent properties such as large specific surface area was employed in constructing electrochemical sensors because of its unusual properties such as low cost, wide potential window, good biocompatibility, relatively inert electrochemistry and high electrical conductivity [1]. Metal nanoparticles (NPs) possess several advantages in terms of electroanalysis such as large specific surface area, good biocompatibility, excellent catalysis, control over local microenvironment etc [2]. Metal NP decorated Gr sheets has drawn the attention of researchers in the field of electrochemical sensors as the Gr-based metal nanocomposites can display a synergistic effect of catalytic character of metal NPs and high electrical conductivity of Gr [1]. Au NPs are known for their unique optical and surface properties that attract a great deal of attention because of their potential applications in catalysis, optics, sensing, nanobiotechnology etc [3]. The metal NP-Gr composites are usually obtained from in situ reduction of metallic salts on graphene oxide (GO)/modified Gr sheets [4, 5, 6] using externally added reducing or stabilizing agents or both. Muszynski et al. [7] have reported the synthesis of Gr sheets decorated with gold (Au) NPs by chemically reducing $AuCl_4^-$ with $NaBH_4$ in a Gr-octadecylamine suspension. Goncalves et al. [5] have reported the surface modification of Gr nanosheets with Au NPs based on the reduction of Au (III) complex by sodium citrate. These reduction methods have advantages of large-scale and high yield, but the use of excessive reducing agents will leave lots of chemical residues. Hence a simple and environmental friendly method for the synthesis of Gr-based metal nanocomposites is favored.

Recently, Tian et al. reports [8] the preparation of Au NPs–β-cyclodextrin (CD)–Gr (AuNPs–CD–Gr) by in situ thermal reduction of GO-CD and $HAuCl_4$ with sodium hydroxide (NaOH). The Au NPs are known to electrochemically oxidize glucose in alkaline solutions [9] and has used for the simultaneous determination of Ascorbic acid (AA), dopamine and uric acid with AuNPs–CD–Gr modified electrode by square wave voltammetry, whereas Kong et al. [10] reports a GO-thionine-Au nanostructure composite (GO–THi–Au/GCE) as a non-enzymatic glucose sensor with a detection limit of 0.05 μM.

In this paper, we present the preparation of gold nanoparticle functionalized graphene (Au-Gr) nanocomposites in aqueous medium using a simple, green synthesis method which utilizes the biocompatible, non-toxic CD [11] as the reducing agent for Au (III) ions. Reduced graphene oxide functionalized with CD molecules, named as CD-Gr, is used as the substrate to reduce and anchor Au (III) ions to form Au-Gr. Functionalization of Gr by CD renders Gr dispersible in water and its aqueous suspension yields individual Gr nanosheets of ~2 nm thickness and the CD

acts as reducing agent as well as capping agent for the Au-Gr/Ag-Gr [12-15]. Our electrochemical sensing studies using the Au-Gr nanocomposite as a non-enzymatic electrode indicates that Au-Gr possesses excellent electrochemical sensing properties better than the previously reported AuNPs–CD–Gr and is attributed to the usage of Gr which renders better conductivity. The non-enzymatic electrodes are highly desirable because it offers higher stability, simplicity, reproducibility compared to the enzymatic counterparts. In this paper we have employed Au-Gr for the first time for sensing glucose and the results indicate that the synergistic effect of Au NPs and Gr makes this nanocomposite an excellent material for sensing of glucose. Our results indicate that the Au-Gr possesses the best detection limits for glucose and AA, with 10 and 40 nM respectively, compared to the values reported in the literature.

2. Experimental

2.1 Raw materials

Graphite (21 μm particle size) and CD (97%) and hydrogen tetrachloroaurate (III) ($HAuCl_4$) were purchased from Sigma Aldrich India Co. Ltd. CD was recrystallized before use. DMF, DMSO, potassium permanganate ($KMnO_4$), hydrogen peroxide (H_2O_2), hydrochloric acid (HCl), sulfuric acid (H_2SO_4), NaOH, di-sodium hydrogen phosphate dihydrate, sodium dihydrogen phosphate monohydrate, Glucose anhydrous and AA were purchased from Merck, India Ltd. Distilled water was used in all the procedure unless specified otherwise.

2.2 Characterization

Universal Attenuated Total Reflection (UATR) mode of Fourier Transform Infrared (FTIR) spectroscopy was used for recording IR spectra using Perkin Elmer spectrum100 spectrophotometer. WI Tec alpha 300R instrument was used for performing the Raman characterizations of samples, wavelength used is 532 nm. The Raman spectrometer used was a 300 mm focal length Acton SP3200 fitted with triple grating. XRD pattern was characterized using Xpert-pro diffractometer using Kα wavelength (1.54 Å) of Cu metal. Thermogravimetric analysis (TGA) was performed using TA Q50. Absorption spectra were recorded by CARY 100 Bio UV-Visible spectrophotometer. Agilent 5500 Scanning Probe Microscope Atomic force microscopy (AFM) with 9 μ scanner was used in tapping mode for AFM imaging. Scanning electron microscopy (SEM) was performed on a Zeiss EVO 18 Scanning electron microscope with an acceleration voltage of 15 kV. Transmission electron microscopy (TEM) analysis was done using JEOL JEM-2100 microscope with the acceleration voltage of 200 kV.

2.3 Preparation of GO and Gr

The GO was synthesized according to modified Hummers' method [16]. Preparation of Gr from GO was done using hydrazine hydrate reduction, which was described elsewhere [17].

2.4 Preparation of CD-Gr

In a typical synthesis of CD-Gr, Gr (20 mg) and 100 mg of recrystallized CD were taken in an agate mortar and crushed by adding distilled water (1 ml) using a pestle for 3 hours. Distilled water was added in drops whenever the mixture became dry. After three hour of crushing, the powder obtained was dialysed in distilled water for 1-2 days and then centrifuged to remove water and dried in a vacuum oven at 60 ^oC overnight.

2.5 Preparation of Au-Gr

In a typical synthesis of the Au-Gr nanocomposite, 10 ml of $HAuCl_4$ (1 mM) solution was heated and to the boiling solution, 3-6 ml of 0.01 % CD-Gr dispersion was added. The solution was boiled for another 30 minutes, till a color change due to the formation of Au NPs was observed.

2.6 Electrochemical methods

The electrochemical behaviors of glucose and AA (in 0.1 M NaOH and 0.1 M Phosphate buffer solution respectively) at the three different electrodes were investigated by cycle voltammetry (CV). The three electrodes include Gr, CD-Gr and Au-Gr (0.5 mg/ml suspension each in DMF) drop casted glassy carbon electrodes (GCE). All the voltammetric determinations were performed on an Autolab (PGstat320N from Metrohm) electrochemical workstation. All the experiments were carried out in a conventional electrochemical cell containing a drop casted GCE working electrode, a platinum wire counter electrode and an Ag(s)/AgCl(s)/Cl^-(aq.) (saturated KCl) as reference electrode. All the experiments were performed at room temperature.

2.6.1 Preparation of electrodes for sensing

Prior to preparation of the electrode for sensing studies, a GCE was mechanically polished with wetted microcloth containing alumina powder, and then carefully cleaned in distilled water by ultra-sonication for 2 minutes. After each analysis, the GCE was cleaned using DMF followed by distilled water by ultrasonication for 2 minutes each. The samples (Gr, CD-Gr, or Au-Gr) dispersed in DMF were drop casted over the pre-treated GCE carefully and then allowed to dry for 24 hours at room temperature. DMF was used because it was able to disperse all the above mentioned samples.

3. Results and Discussion

3.1 Formation and Characterization of CD-Gr

The formation of the CD-Gr was confirmed by various techniques such as FTIR & Raman spectroscopy, TGA, SEM and AFM. The FTIR and Raman spectra of the GO, Gr and CD-Gr are given in Figure S1 (supplementary info). The FTIR of the CD-Gr showed the peaks of CD and the Raman spectra confirmed the presence of Gr in the CD-Gr. The thermogram (Figure S2) of the CD-Gr showed the presence of CD.The AFM analysis of the CD-Gr dispersions in water, made by ultra-sonicating for 30 minutes, showed Gr nanosheets of ~ 2 nm thicknesses (Figure S3). Proposed scheme for the formation and structure of the CD-Gr, and Au-Gr from CD-Gr are illustrated in Figure 1. The thickness of the individual layer of Gr sheet is 0.354 nm and the height of CD is 1.53 nm. Therefore the

thickness of ~2 nm observed in our analysis can be attributed to the presence of CD molecules on the individual Gr sheets which agrees with previous reports [18].

3.2 Formation and Characterization of Au-Gr

The Au-Gr was prepared from the CD-Gr and the formation of the Au-Gr was confirmed by various techniques. The thermogram of the Au-Gr (Figure S2) showed an increase in the residual weight from that of the CD-Gr indicating the presence of Au in the Au-Gr. Further characterization of the Au-Gr composite by SEM and TEM (Figure 2) clearly showed the presence of Gr and Au NPs in the composite. The SEM images clearly showed the presence of Au NPs attached to Gr sheets and the images revealed that the Au NPs were not aggregated and uniformly distributed throughout the Gr sheets. The TEM images agreed with this observation. The non-aggregation of Au NPs might possibly be attributed to the presence of CD on the Gr sheets which reduces the Au (III) ions to Au NPs and stabilizes the formed NPs. The TEM images of the Au-Gr revealed the presence of Gr nanosheets and Au NPs of 50-150 nm in size. The EDAX spectrum of the Au-Gr showed the presence of Au, carbon and oxygen in the Au-Gr and thus confirmed the formation of Au-Gr. The Au-Gr was further characterized by XRD and the pattern showed the peaks corresponding to Au. The diffraction peaks at 2θ = 38.2◦, 44.4◦, 64.6◦ and 77.5◦ could be indexed to the (1 1 1), (2 0 0), (2 2 0) and (3 1 1) planes of a pure face-centered crystalline structure of Au [19]. The thin CD-Gr sheets as evident from the AFM images and that of Au-Gr from the TEM and the absence of the broad characteristic peak of rGO around 26 ^{0} suggest that the Gr sheets are well separated by the Au NPs in the Au-Gr. Based on these results we suggest that each Gr sheet is attached with Au NPs and are not aggregated in the Au-Gr nanocomposite. The UV-Visible spectroscopy is an important tool for characterizing metal NPs and the spectrum of the Au-Gr showed the characteristic surface plasmon resonance (SPR) peak of Au NPs at around 550-560 nm and thus confirmed the formation of Au NPs. Thus, the characterization results undoubtedly confirm the formation of Au NP functionalized Gr nanocomposite from the CD-Gr.

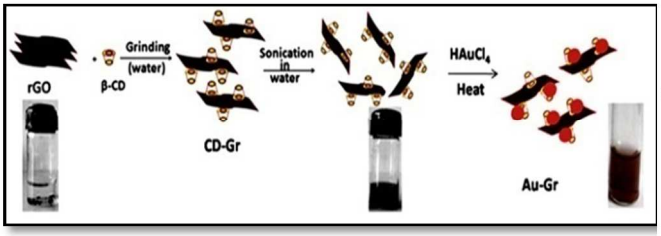

Figure 1. Schematic of the formation of CD-Gr, and Au-Gr from the CD-Gr. (Inset digital images of Gr, CD-Gr and Au-Gr in water)

Heating of $HAuCl_4$ in presence of the physical mixture of Gr and CD resulted in a black precipitate and did not yield the color of Au NP and the resulting solution did not show the SPR peak of Au NPs. The result suggested that the mixture of CD and Gr did not form Au NP in the described condition or this might be due to the lack of stabilization of Gr sheets and the formed Au NPs, which undergo aggregation, resulting in a non-dispersible black precipitate, which leads to the the absence of the color and the SPR peak. The mechanism of formation of the Au-Gr can be explained as follows: the Au (III) ions gets attached to the –OH groups of CD and the CD reduces the Au (III) ions to Au NPs thus resulting in the formation of Au-Gr. The non-occurrence of the color of Au NP in the same conditions with Gr and CD mixture suggest that the functionalization of Gr by CD is crucial in the formation of the dispersible Au-Gr under the suggested conditions.

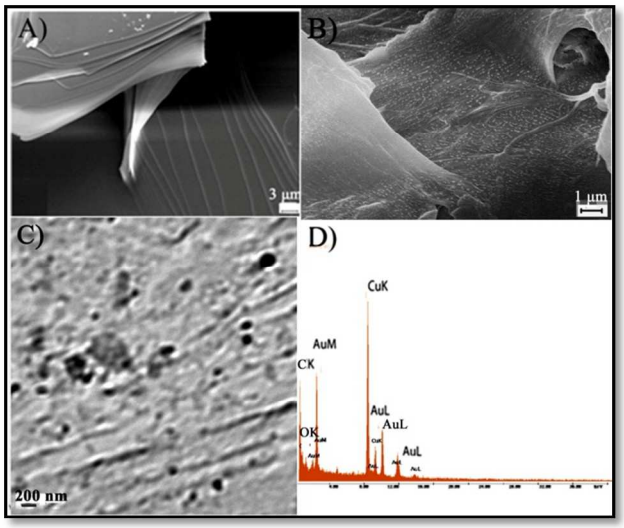

Figure 2. SEM image of (A): CD-Gr and (B): Au-Gr; (C) and (D): TEM image and the EDAX spectrum of the Au-Gr.

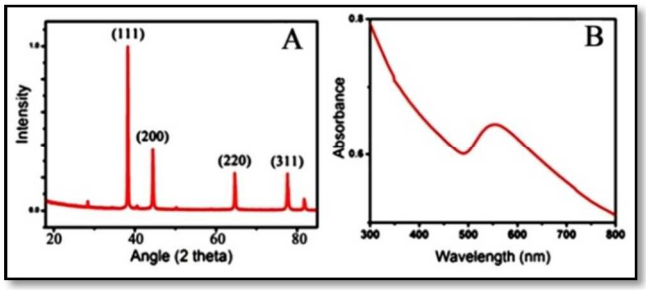

Figure 3. (A): XRD pattern and (B): UV-Visible spectrum of the Au-Gr

3.3 Electrochemical Sensing properties

One of the potential applications of Au NP functionalized Gr is in electrochemical sensing of analytes. It is known that Au NPs can electrochemically oxidize glucose in alkaline solution; however Au NPs tend to aggregate and has poor adsorption properties to the hydrophobic GCE [9]. Recently, Gr based materials has been extensively studied as electrode materials for sensing various analytes. Therefore, we investigated the electrochemical sensing property of Au-Gr as a non-enzymatic electrode for sensing glucose and further extended it to sense AA.

3.3.1 Electrochemical behavior of Glucose

In an attempt to study the electrochemical sensing properties of the electrodes, the electrochemical oxidation of glucose in 0.1 M NaOH was investigated by cyclic voltammetry (CV) at the three different electrodes: Gr coated GCE (Gr/GCE), CD-Gr coated

GCE (CD-Gr/GCE) and Au-Gr coated GCE (Au-Gr/GCE). The results of the CV experiments are given in Figure 4A and Figure S6. The CV curve of glucose at the Au-Gr/GCE exhibited three clear electrochemical processes during the anodic sweep and one during the cathodic return sweep. However, no redox peaks were observed for glucose at the Gr/GCE and CD-Gr/GCE for the same concentration (Figure S6A). The first peak at around -0.02 V (Figure 4C, peak "a") was attributed to the dehydrogenation of anomeric carbon under adsorption control [9]. A second oxidation peak was observed at around 0.2 V (Figure 4C, peak "b") and was attributed to the formation of gluconate from glucose oxidation and the third peak around 0.45 V (Figure 4C, peak "c"), indicated the occurrence of Au surface oxidation [9]. The Au-O was then reduced at 0.1 V (Figure 4C, peak "d") during the cathodic scan [9]. The interesting aspect of glucose on Au NP electrode is the oxidation peak of glucose during the cathodic scan which was obtained as soon as the oxide layer of Au was reduced [20-22]. The mechanism for the oxidation during the cathodic sweep was first proposed by Liu and Makovos: the oxide layer is reduced to generate free O^{2-} anions which react with glucose to give gluconic acid, and then the Au surface undergoes re-oxidation by OH^- in solution [20]. The corresponding peaks were not detected at the Gr/GCE and CD-Gr/GCE electrodes even at 3 mM and this proves the inferior electroactivity of the electrodes towards the oxidation of glucose compared to that of the Au-Gr/GCE. A small peak started appearing for glucose at both the electrodes (Gr/GCE and CD-Gr/GCE) from 3.2 mM onwards.

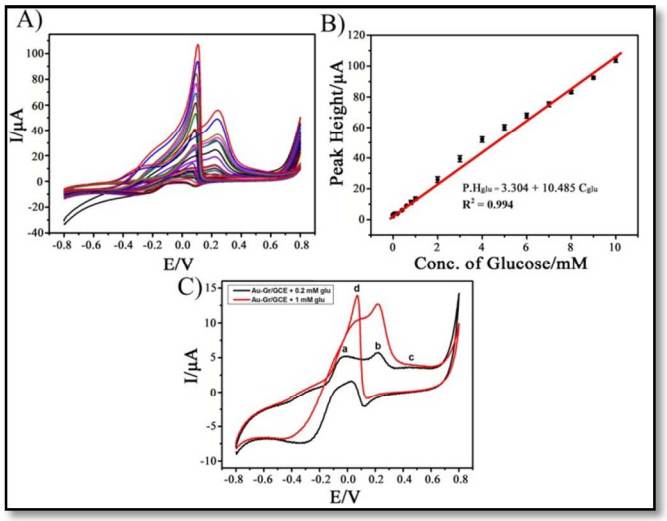

Figure 4. (A): CV scans of glucose at the Au-Gr/GCE for the concentration range of 0 to10 mM and (B): The corresponding linear relation between peak height and concentration from 10 nM to10 mM. (C): CV scans of glucose using the Au-Gr/GCE in 0.1 M NaOH for two different concentrations (0.2mM and 1mM); the peaks a, b, c and d correspond to the formation of different electrochemical oxidation and reduction products of glucose and Au .

The response of the Au-Gr/GCE sensor for glucose was tested over the concentration range of 10 nM – 10 mM. As shown in Figure 4B, excellent linearity was achieved (R^2 = 0.994) throughout this concentration range, while such a response was absent with the other two electrodes (GCE/Gr and GCE/CD-Gr). As illustrated in Figure S6, the observed detection limit of glucose using Au-Gr/GCE was 10 nM of, where as GCE/Gr and GCE/CD-Gr did not show any glucose detection in the nanomolar and micromolar range. The results clearly demonstrate the enhanced electrochemical sensing behavior of Au-Gr towards glucose biomolecule. Ideally, for Gr to preserve its distinct properties, its use should be narrowed to single or few-layer morphology [34]. Here, owing to the functionalization of CD, Gr is restricted to one layer thickness, which might be a major reason for the higher sensitivity exhibited by the Au-Gr. However, it is well known that Gr sheets tend to form irreversible agglomerates because of the van der Waals interactions and even restack to form multi layers over the electrode surface in dry state [35]. The prevention of restacking by the NPs as spacers will result in the increase in the surface area and thereby the enhancement in performance. Due to the same reason, Au-Gr possesses high surface area leading to high analyte loading and increased sensitivity [34]. Electrodes made from thin Gr sheets have significantly uniform distribution of electrochemically active sites, and its entire volume is exposed to the surrounding due to its 2D structure, making it very efficient in detecting adsorbed molecules [34]. Materials such as Au generally exhibit poor biomolecule adsorption which results in weak substrate-biomolecule coupling and high noise [34]. Gr can enhance the adhesion of biomolecules due to the π-stacking interactions between its hexagonal cells and the carbon based ring structures widely present in bio/nano molecules.

NPs are known to increase the stability and maintain the activity of biomolecules, enhance the catalysis of electrochemical reactions, decrease overpotentials and enable the reversibility of redox reactions. The conductivity of NPs enhances the electron transfer between the active centres of biomolecules and electrodes so that the particles can act as electron transfer conduits or mediators [34]. A major shortcoming of NPs is their lack of stability and tendency to aggregate. Immobilization of NPs is crucial for developing electrocatalytic devices [34]. In Au-Gr these limitations are overcome due to the tethering of Au NPs to the Gr substrate through CD molecules thus enhancing the stability of the electrode. It is evident that the Au NPs are not aggregated in the Au-Gr from the SEM and TEM images of the Au-Gr. Bare Au NP on the GCE has limitations such as aggregation and lower adhesion [9]. However, in Au-Gr the hydrophobic nature of Gr provides improved adhesion to the GCE. This will prevent the easy detachment of the sensor from the surface of the electrode thus improving the stability of the electrode. Our studies show that Au-Gr/GCE retains the 100 % current response even after three weeks of storage at room temperature and the result proves the excellent stability of the non-enzymatic glucose sensor. Non-enzymatic glucose sensors based on the electrocatalytic oxidation of glucose is a subject of intense research interest, as it can avoid the poor stability of enzymatic sensors and the interference of certain electro-oxidizable species [23]. Our results show that the Au-Gr composite offers in addition to the excellent sensing property, stability as well. This is the first time, Au NP functionalized Gr is tested as a non-enzymatic sensor for electrochemically detecting glucose molecule and the results show that the Au-Gr possesses

excellent sensing properties, better than any other reported non-enzymatic and enzymatic electrodes and is attributed to the synergistic effect of Au NP and Gr.

A comparison of the reported values for sensing glucose using other electrodes and our results are given in Table 1. The result shows that the Au-Gr exhibits the best detection limit compared to all other values and has linearity in the physiological glucose level. The rate of electron transfer has been shown to be surface dependent. The creation of specific surface functional groups can increase this rate significantly [34]. The surface functional groups in the Au-Gr due to the CD molecules can possibly enhance the adsorption and desorption of molecules. The superior electrocatalytic property of the Au-Gr is attributed to the synergistic effect of the catalytic properties of nanocrystalline Au particles and the improved surface area, adsorption and conductivity offered by thin Gr sheets. The CD molecules mainly contribute to the atomic nature of Gr sheets thus enhancing the conductivity, surface area and electron transfer of Gr sheets and in addition improve the adsorption of biomolecules. In order to see the potentiality and versatility of the Au-Gr as a non-enzymatic sensing electrode material we investigated the electrochemical sensing of the Au-Gr towards another important biomolecule, AA.

3.3.2 Electrochemical behavior of AA

The electrochemical oxidation of AA was conducted in 0.1 M Phosphate buffer solution and investigated by CV. The experimental results show that the Au-Gr/GCE exhibits excellent electrochemical sensing properties compared to that of the Gr/GCE and CD-Gr/GCE. (Figure S7A).

The CV response of Au-Gr/GCE sensor against increasing concentration of AA is illustrated in Figure 5A. The plot clearly showed the enhancement of the peak current, corresponding to the electrochemical oxidation of AA, with the increasing concentration of AA.

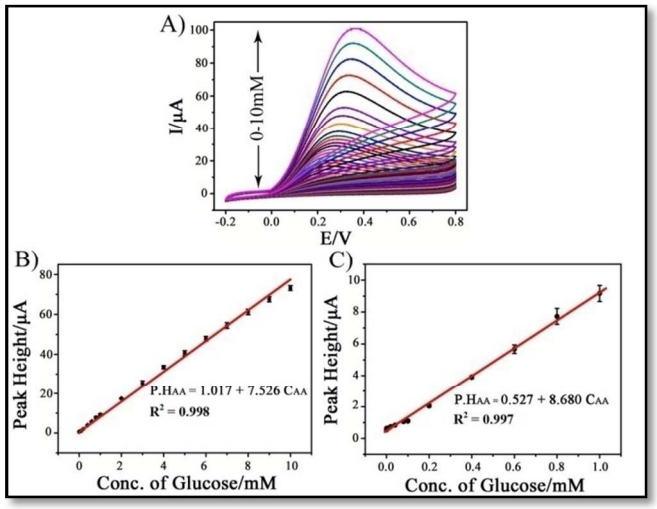

Figure 5. (A): CV scans of AA at the Au-Gr/GCE for the concentration range of 0 to 10 mM (B) and (C): Corresponding linear relation between peak height and concentration for the concentration ranges, 40 nM to 10 mM and 40 nM to 1 mM (lower range linearity), respectively.

As shown in Figure 5B, the Au-Gr/GCE gave an excellent linearity in a concentration range of AA from 40 nM to 10 mM ($R^2 = 0.998$), the experimental range studied was 10 nM -10 mM. Moreover at lower concentration range (40 nM – 1 mM) of AA, Au-Gr/GCE showed a remarkable enhancement in current response and with good linearity as illustrated in Figure 5C. Such a good linear response was absent with Gr/GCE and CD-Gr/GCE sensors (Figure S7A). The detection limit of the Au-Gr/GCE towards AA was found to be 40 nM, whereas those of the Gr/GCE and CD-Gr/GCE were 0.2 and 0.6 mM, respectively. The better performance of the Au-Gr/GCE towards AA molecule compared to that of the Gr/GCE and CD-Gr/GCE can be attributed to the synergistic effect of the catalytic activity of Au NPs [24] and the excellent conductivity, better adsorption and higher surface area of Gr in the composite and is explained in the glucose section. The result is found to be one of the best when compared to other AA electrochemical sensors reported previously (Table 2). The reported detection limit of AA for the previously reported Au NPs functionalized Gr through CD [8] was 10 μM where as our value is 40 nM.

Our results show that, the detection limits obtained for glucose and AA are 10 and 40 nM respectively and are the best values reported so far. The better performance of the Au-Gr electrode towards AA when compared to the previously reported Au-CD-GR [8] is possibly due to the improved conductivity offered by the Gr counterpart as Gr prepared by hydrazine hydrate reduction is used in our work. The low electrical resistance and atomic thickness of Gr, enhance the electrochemical sensing [34].The Nyquist plots obtained for the Au-Gr, CD-Gr and Gr are given in Figure S7B, which show that the interfacial charge resistance is minimal and the materials have good conductivity. Moreover, as the Au-Gr disperses well in water and DMF (Figure 1 inset) the homogeneity induced by the CD molecules may play a role in the improved sensing property. The anchoring of Au NPs through CD molecules might decrease the aggregation and increase the proximity of Au NPs to Gr and thus increases the electron transfer rates.

Thus the enhanced current response offered by the Au-Gr/GCE was assigned to the synergistic effects of Gr, CD and Au NPs (high conductivity, surface area, adsorption and catalytic activity). Zhang et al reported [24] that Au NPs may act as catalysts for AA oxidation. Gr based electrochemical sensors had been studied and proven as potential candidates for sensing many analytes due to their better conductivity and higher surface area. When compared to the previous reports [8, 10], the performance of the Au-Gr is far better in terms of sensing property and detection limit (10 and 40 nM respectively) towards glucose and AA.

Table 1. The comparison of linearity range and detection limit of glucose by Au-Gr/GCE with other reported literature values of enzymatic and nonenzymatic sensors.

Type of electrode	Linear range (mM)	Detection limit (μM)	Ref.
Chitosan (CHI)–Au NPs / GCE	0.4-10.7	370	[25]
AuNPs/GCE	0.1 - 25	50	[26]
Au NW array electrode	0.5-14	30	[27]
GO–THi–Au/GCE	0.2 -13.4	0.05	[10]
Gr/AuNPs/GOD/ CHI (enzymatic)	2 - 10	180	[30]
Gr/nano-Au/GOD/GCE (enzymatic)	0.2-2 and 2-20	17	[1]
PtNi NP-Gr	Up to 35	10	[28]
Au-Gr/GCE	0.00004 -3 (R^2= 0.994) & 4-10 (R^2= 0.991)	≤ 0.01	Our result

Table 2. The comparison of linearity range and detection limit of AA by Au-Gr/GCE with other reported literature values of enzymatic and nonenzymatic sensors.

Type of electrode	Linear range (mM)	Detection limit (μM)	Ref.
GC/GO1	0.1-10	-	[29]
Au NPs-L-cysteine	0.008–5.5	3	[32]
CHI-Gr/GCE	0.050–1.2	50	[33]
Au NPs-CD-Gr/GCE	0.030–2	10	[8]
Gr–poly(3,4-ethylenedioxy-thiophene)/ ascorbate oxidase	0.005–0.48	2.0	[31]
Au-Gr/GCE	0.00004 -10	0.04	Our result

4. Conclusions

A successful green method for the preparation of Au-Gr from CD-Gr is reported. The CD-Gr in water yields Gr nanosheets of ~2 nm thickness and the CD molecules act as stabilizing and reducing agent for the Au NPs. Gr is used as the starting material for preparing CD-Gr. The method uses water as solvent and CD as reducing agent and hence is environmental friendly. Importantly, our results suggest that the Au-Gr exhibits excellent non-enzymatic electrochemical sensing properties with the best detection limits towards glucose and AA molecule (10 and 40 nM, respectively), compared to the literature values. The better sensing of the Au-Gr towards AA compared to that of the previously reported Au-CD-Gr is assigned to the better conductivity of Gr, facilitated by the usage of Gr made by hydrazine hydrate reduction. Our results suggest that our Au-Gr is better in terms of electrochemical sensing properties and is attributed to the better electron transfer and transport by the atomic thin Gr sheets obtained by the functionalization of CD. The synergistic effect of the catalytic activity, higher surface area, adsorption and conductivity of Au NPs and Gr and the better adsorption and homogeneity induced by CD enhances the electrochemical performance of the Au-Gr and makes it a potential candidate for sensing applications.

Notes and references

Department of chemistry
Indian Institute of Space Science and Technology,
Thiruvananthapuram
Kerala- 695 547
India
**Corresponding author. Tel.: +914712568537; Fax: +914712568541.*
E-mail: sandhya@iist.ac.in (K.Y. Sandhya).

† Electronic Supplementary Information (ESI) available: [FTIR spectra, Raman spectra, TGA, additional AFM, SEM & TEM images, CV reponses are given in the supplementary information]. See DOI: 10.1039/b000000x/

1 X. Wang and X. Zhang, *Electrochimica Acta*, 2013, **112**, 774-782.
2 C.M. Welch, R.G. Compton, *Anal. Bioanal. Chem*, 2006, **384**, 601.
3 C. M. Shen, C.Hui, T. Z.Yang, C. W. Xiao, J. F. Tian, L. H. Bao, S.T. Chen, H. Ding and H. J. Gao, *Chem. Mater*., 2008, **20**, 6939.
4 C. Xu, X. Wang and J. W. Zhu, *J. Phys. Chem. C*, 2008, **112**, 19841.
5 G. Goncalvest, P. A. A. P. Marques, C. M. Granadeiro, H. I. S. Nogueira, M. K. Singh and J. Gracio, *Chem. Mater*., 2009, **21**, 4796.
6 X. Z. Zhou, X. Huang, X. Y. Qi, S. X. Wu, C. Xue, F. Y. C. Boey, Q. Y. Yan, P. Chen and H. Zhang, *J. Phys. Chem. C*, 2009, **113**,10842.
7 R. Muszynski, B. Seger and P. V. Kamat, *J. Phys. Chem. C*, 2008, **112**, 5263.
8 X. Tian, C. Cheng, H. Yuan, J. Du, D. Xiao, S. Xie and M. M. F.Choi, *Talanta*, 2012, **93**, 79– 85.
9 M. Pasta, R. Ruffo, E. Falletta, C.M. Mari and C.Della Pina, *Gold Bulletin*, 2010, **43**, 1.
10 F. Y. Kong, X. R. Li, W. W. Zhao, J. J. Xu and H. Y. Chen, *Electrochemistry Communications*, 2012, **14**, 59–62.
11 K. Liu, H. Fu, Y. Xie, L. Zhang, K. Pan and W. Zhou, *J. Phys. Chem. C*, 2008, **112**, 951-7.
12 J. Bai , Q. Yang, M. Li , S. Wang, C. Zhang and Y. Li, *Materials Chemistry and Physics*, 2008, **111**, 205–208.
13 P. R. Gopalan, A. G. Annaselvi, and P. Subramaniam, International *Journal of Nanomaterials and Biostructures*, 2013, **3**, 26-30.
14 T. Huang, F. Meng and L. Qi, *J. Phys. Chem. C*, 2009, **113**, 13636–13642.
15 S. Manivannan and R. Ramaraj, *Pure Appl. Chem*., 2011, **83**, 2041–2053.
16 G. Venugopal, K. Krishnamoorthy, R. Mohan, S.J. Kim, *Materials Chemistry and Physics*, 2012, **132**, 29-33.
17 S. Stankovich, D. A. Dikin, R. D. Piner, K. A. Kohlhaas, A. Kleinhammes and Y. Jia et al., *Carbon*, 2007, **45**, 1558-65.
18 Y. Guo, S. Guo, J. Ren, Y. Zhai, S. Dong and E. Wang, *ACS nano*. 2010, **4**, 4001-10.
19 X. Feng, J. Hu, X. Chen, J. Xie and Y. Liu, *J. Phys. D: Appl. Phys*. 2009, **42**, 042001 (6pp).
20 M. W. Hsiao, R. R. Adzic and E.G. Yeager, *J. Electrochem. Soc*., 1996, **143**, 759.
21 C. Xiang, Q. Xie and S. Yao, *Electroanalysis*, 2003, **15**, 987.
22 B. K. Jena and C. R. Raj, *Chem. Eur. J*., 2006, **12**, 2702.
23 H. F. Cui, J. S. Ye, W. D. Zhang, C. M. Li, J. H. T. Luong and F. S. Sheu, *Anal. Chim. Acta*, 2007, **594**, 175.
24 L. Zhang, H. W. Shi, C. Wang and K. Y. Zhang, *Microchim Acta*, 2011, **173**, 401–406.
25 D. Feng, F. Wang and Z. Chen, *Sensors and Actuators B*, 2009, **138**, 539–544.
26 G. Chang, H. Shu, K. Ji, M. Oyama, X. Liu and Y. He, *Applied Surface Science*, 2014, **288**, 524– 529.

27 S. Cherevko and C. H. Chung, *Sensors and Actuators B,* 2009, **142** 216–223.
28 H. Gao, F. Xiao, C. B. Ching and H. Duan, *ACS Appl. Mater. Interfaces,* 2011, **3**, 3049–3057.
29 D. V. Stergiou, E. K. Diamanti, D. Gournis and M. I. Prodromidis, *Electrochemistry Communications*, 2010, **12**, 1307–1309.
30 C. Shan, H. Yang, D. Han, Q. Zhang, A. Ivaska and L. Niu, *Biosensors and Bioelectronics,* 2010, **25**, 1070–1074.
31 L. Lu, O. Zhanga, J. Xu, Y. Wena, X. Duan, H. Yu, L. Wu and T. Nie, *Sensors and Actuators B*, 2013, **181**, 567– 574.
32 G. Hu, Y. Ma, Y.Guo and S. Shao, *Electrochimica Acta*, 2008, **53**, 6610–6615.
33 D. Han, T. Han, C. Shan, A. Ivaska and L. Niu, *Electroanalysis*, 2010, **22**, 17-18, 2001 – 2008.
34. M. S. Artiles, C. S. Rout and T. S. Fisher, *Advanced Drug Delivery Reviews*, 2011, **63**, 1352–1360
35. T. T. Baby, S.S. J. Aravind, T. Arockiadoss, R.B. Rakhi and S. Ramaprabhu, *Sensors and Actuators B,* 2010, **145**, 71–77